Facile large-scale synthesis of monodisperse Fe nanoparticles by modest-temperature decomposition of iron carbonyl

doi: 10.1063/1.2711391

Facile large-scale synthesis of monodisperse Fe nanoparticles by modest-temperature decomposition of iron carbonyl

Haitao Yang,[a] Fumiyuki Ito, Daiji Hasegawa, and Tomoyuki Ogawa
Department of Electronic Engineering, Graduate School of Engineering, Tohoku University, Aoba-yama 05, Sendai 980-8579, Japan

Migaku Takahashi
New Industry Creation Hatchery Center, Tohoku University, Aoba-yama 10, Sendai 980-8579, Japan

(Presented on 9 January 2007; received 30 October 2006; accepted 12 December 2006; published online 9 May 2007)

A facile synthesis method for monodisperse Fe nanoparticles has been developed by the injection of iron carbonyl into kerosene at a modest temperature, typically 180 °C. By controlling the reaction time, the molar ratio of surfactants to $Fe(CO)_5$, and the $Fe(CO)_5$ concentration in kerosene, 3–12 nm monodisperse Fe nanoparticles were prepared. The size distribution is very narrow and any size-selective treatment is not required even when several grams of Fe nanoparticles are synthesized in one pot. Magnetic measurements reveal that the saturation magnetization (M_s) of the 9.3 nm Fe nanoparticles is always over 150 emu/g at room temperature. © *2007 American Institute of Physics*. [DOI: 10.1063/1.2711391]

I. INTRODUCTION

Recent improvements in electronic devices have led to demand for further miniaturization and higher-frequency operation of magnetic devices.[1,2] To improve the ferromagnetic response in the high-frequency range, the ferromagnetic resonance frequency of conventional ferromagnetic materials has to be increased by induced magnetic anisotropy, which results in a lack of isotropic magnetic properties in the high-frequency range. Superparamagnetic metallic nanoparticles (NPs) assemblies with high saturation magnetization (M_s), such as Fe and $Fe_{70}Co_{30}$, can realize high susceptibility and permeability and can thus become good candidates for use as high-frequence magnetic materials, since superparamagnetic NPs have isotropic magnetic properties and no hysteresis loss. For the chemical synthesis of Fe NPs, the decomposition of iron carbonyl is frequently used, largely due to the ease of use and the lack of by-products for this reaction.[3–5] However, a widely used synthesis procedure is the decomposition of $Fe(CO)_5$ at very high temperature such as 290 °C for a long time, in which large amounts of iron oxide easily form on the surface of Fe NPs. The magnetization of NPs with a size less than 16 nm is usually less than 130 emu/g.[6] Moreover, in most syntheses reported so far, only microgram quantities of monodisperse NPs were produced with size-selective treatment in a reaction.

Here, we report the large-scale synthesis of monodisperse Fe NPs using inexpensive surfactants and organic solvents as reactants. We were able to synthesize as much as 2 g of monodisperse NPs in a single reaction, without the need for a size-sorting process. Moreover, the particle size could be controlled simply by varying the experimental conditions. The magnetic properties of Fe NPs, including saturation magnetization at different temperatures and sizes of the NPs, were investigated.

II. EXPERIMENT

The synthesis and other treatment processes were carried out in a glovebox with 1–5 ppm of O_2 and H_2O. All commercially available reagents were purchased from Aldrich. Kerosene was purified by carefully degassing using a freeze-pump-flaw technique before use. In a typical synthesis of 2 g Fe NPs with a size of 9.0 nm, 40 mmol oleyl amine (OY) and 400 ml kerosene were added into a flask and continuously heated to a temperature of about 180 °C. 40 mmol $Fe(CO)_5$ was injected during vigorous stirring. The black dispersion was vigorously stirred for 60 min and the black reaction mixture was then cooled to room temperature. The black product was precipitated by adding ethanol to the dispersion. The supernatant was discarded by centrifugation. The particles were redispersed in hexane with about 50 μl of oleyl amine to ensure stability.

Transmission electron microscopy (TEM) (JEOL 3010 at 300 kV) was employed to determine the morphology, size, and size distribution of the Fe NPs. Samples were formed by drying hexane dispersions of particles on amorphous-carbon-coated copper grids and transferred to the TEM chamber as quickly as possible. X-ray fluorescence (XRF) using a Rigaku instrument was used to determine the total amount of Fe from the integrated intensity of fluorescence of the $K\alpha$ line of Fe at 6.40 keV by calibrating the intensities with Fe elemental standard films (purity of 99.99%). Magnetic measurements were conducted using a Quantum Design MPMS-5 superconducting quantum interference device (SQUID) with fields up to 5 T and temperatures from 5 to 300 K.

[a]Author to whom correspondence should be addressed; FAX: +81-22-263-9402; electronic mail: htyang@ecei.tohoku.ac.jp

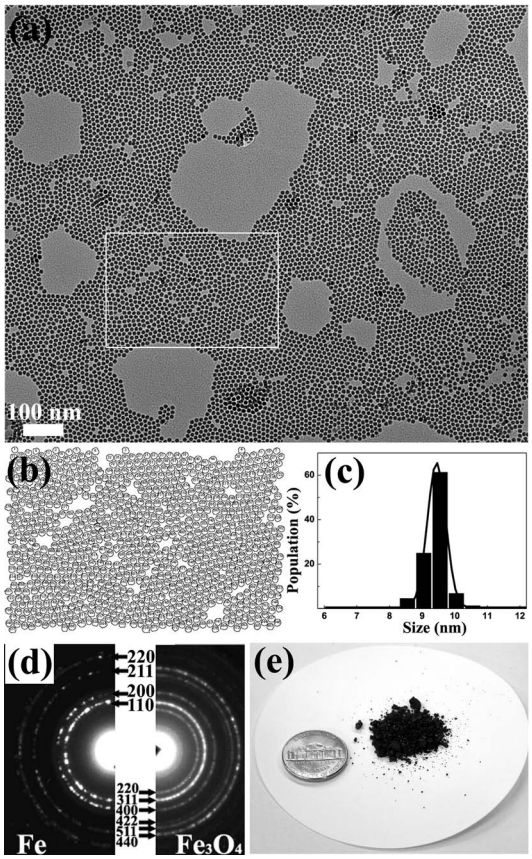

FIG. 1. (a) TEM images of 9.3 nm Fe nanoparticles. (b) Edge outline drawing of particles within the selected rectangular area. (c) The particle size distribution histogram showing that the average diameter of the nanoparticles is 9.3±0.4 nm and the size distribution is a best fit to a log-normal distribution function. (d) bcc Fe diffraction from the (110), (211), (200), and (310) planes can be observed in the electron diffraction patterns. (e) A photograph showing a Petri dish containing 2 g of the monodisperse Fe nanocrystals and a U.S. five-cent coin for comparison.

III. RESULTS AND DISCUSSION

The decomposition of iron carbonyl usually introduces additional nucleation during growth at high temperatures because a range of intermediate iron carbonyls and Fe clusters can form and catalyze the decomposition.[3] The inhibition of additional nucleation during growth is critical for the successful synthesis of monodisperse NPs. Classic studies by La Mer and Dinegar show that the production of monodisperse colloids requires a temporally discrete nucleation event followed by slower controlled growth on the existing nuclei.[7] If the percentage of NP growth during the nucleation period is small compared to subsequent growth, the NPs can become more uniform in size over time.[8] The process conditions required for the synthesis of monodisperse NPs have been applied to the synthesis of uniform-sized Co NPs.[9]

Based on a similar principle, our research group developed a procedure for large-scale synthesis of monodisperse Fe NPs without a laborious size-sorting process. By fast injection of $Fe(CO)_5$ into kerosene at 180 °C, 2 g or more monodisperse Fe NPs could be prepared. Figure 1(a) shows the TEM images of well isolated 9.3 nm Fe nanoparticles with a size distribution of less than 5%. The IMAGEJ 1.3.2J software was used to determine the average particle size and

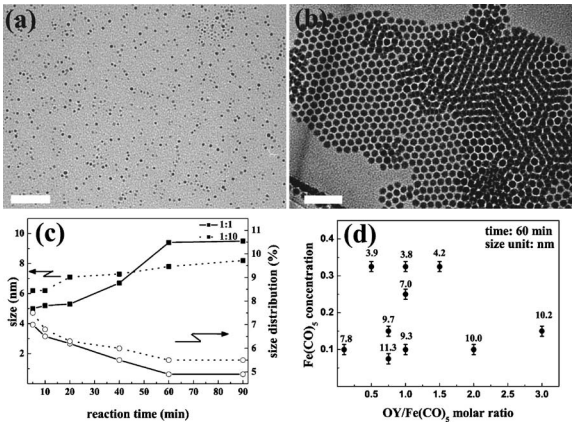

FIG. 2. TEM images of Fe NPs with a size of (a) 4.2 nm and (b) 7.0 nm in which scale bar =50 nm, (c) Influence of reaction time. (d) The molar ratio of surfactants to $Fe(CO)_5$ and $Fe(CO)_5$ concentration in kerosene on the size are summarized here.

the size distribution by analyzing at least 500 particles located in the selected rectangular area in Fig. 1(a). Particles were identified by the contrast between particle and background, and their edges were outlined [as shown in Fig. 1(b)]. The software measured the particle along its major and minor axes, and the particle size was determined as the average of the two. From the particle size distribution histogram [in Fig. 1(c)], the average diameter of 9.3±0.4 nm is obtained. Electron diffraction patterns were used for phase identification of the Fe NPs instead of x-ray diffraction (XRD) patterns due to their high sensitivity to oxidation in air. Figure 1(d) shows electron diffraction patterns of the particles shown in Fig. 1(a) and 10.0 nm Fe_3O_4 NPs. The typical pattern for the Fe NPs consists of four diffraction rings with some spots corresponding to the strongest bcc Fe diffraction from the (110), (211), (200), and (310) planes, which reveals that the Fe NPs have good crystallinity. In the case of Fe_3O_4 NPs, diffraction from a series of crystalline planes such as (220), (311), (400), (422), (511), and (440) was observed. The *d* spacing in these two diffraction patterns was obviously different. Figure 1(e) is a photograph showing a Petri dish containing 2 g of the monodisperse Fe NPs and a U.S. five-cent coin for comparison. The yield evaluated from XRF measurement is about 75% in a typical synthesis procedure.

The particle size can be controlled simply by varying the reaction time, the molar ratio of OY to $Fe(CO)_5$, and the $Fe(CO)_5$ concentration in kerosene. Figures 2(a) and 2(b) show TEM images of Fe NPs with sizes of 4.2 and 7.0 nm. In the case of the 7.0 nm NPs, two or three layer self-assembled structures are observed. Figure 2(c) reveals that the size of the Fe NPs increased with increasing reaction time and the rate of particle growth is different for different molar ratios of OY to $Fe(CO)_5$. The particles obtained are uniform in size and look like spheres at different reaction times. At an $OY/Fe(CO)_5$ molar ratio of 1:1, the size of the particles is smaller within 40 min and a little bigger after 40 min than that of the molar ratio of 1:10. After 60 min, the particle sizes are almost constant in both cases, in other words, the particle growth nearly stops. These results could

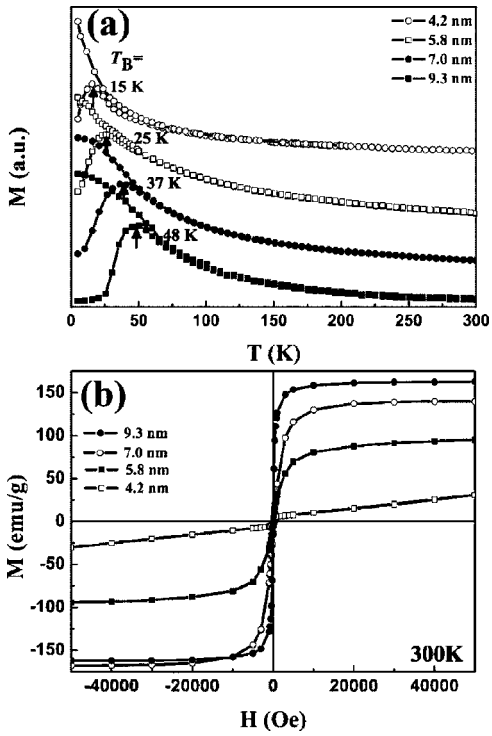

FIG. 3. Zero-field-cooled (lower) and field-cooled (upper) curves of the specific magnetization at 20 Oe field vs temperature for Fe nanoparticles with different sizes. (b) Hysteresis loops for Fe nanoparticles with different sizes at 300 K.

imply that the iron carbonyl decompose at a time to be the nuclei, and then the nuclei are to form larger Fe particles with increasing reaction time. However, even with a extended reaction time of 120 min, the particles did not increase more than around 11 nm. The influence of the molar ratio of OY to $Fe(CO)_5$ and the $Fe(CO)_5$ concentration on particle size is summarized in Fig. 2(d). The $Fe(CO)_5$ concentration in kerosene has a greater influence on the size than the molar ratio of OY to $Fe(CO)_5$. Such behavior is somewhat strange since it is well known that a high ratio of surfactants to reagent favors the formation of more nuclei initially and thus a smaller particle size.[10]

Samples for the magnetic measurements were prepared by adding the concentrated Fe NPs solution in heptane (typically 0.5 vol %) into a quartz tube ($\phi 5 \times 15$ mm^2). The tube was then sealed in a glovebox using Araldite and the diamagnetic background from the quartz tube was subtracted. Such an "ampule" showed no magnetic signal decay even after keeping it in air for a week. Zero-field-cooled (ZFC) and field-cooled (FC) magnetizations as a function of temperature in a 20 Oe field were used to identify the blocking temperature T_B with the maximum in the ZFC curve. Figure 3(a) shows the temperature dependence of magnetization for the Fe NPs in the size range between 4.2 and 9.3 nm. The measured values, $T_B(4.2\ \text{nm})=15$ K, $T_B(5.8\ \text{nm})=25$ K, $T_B(7.0\ \text{nm})=35$ K, and $T_B(9.3\ \text{nm})=48$ K, are qualitatively consistent with the diameter dependence. No Fe oxide signal was observed since they have a high T_B value (usually more than 100 K). Since we focused on the saturation magnetization of Fe NPs at room temperature, the hysteresis loops of the Fe NPs with different sizes at 300 K only are shown in Fig. 3(b). The M_s values of Fe NPs with sizes of 9.3, 7.0, and 5.8 nm were 162.0, 140.0, and 95.0 emu/g, respectively. The M_s of Fe NPs with a size greater than 8.0 nm is always over 150 emu/g at room temperature, which is higher than that of the decomposition of $Fe(CO)_5$ by other groups.[11,12] The relatively high magnetization observed in our experiments can be attributed to good crystallinity of Fe NPs, and a small amount of oxide layer formed during the synthesis process. Good inhibition of oxidation was achieved by doing all the operation in glovebox with Ar gas, and in particular, a weak reduction ability of OY to avoid the introduction of oxidation by surfactants such as oleic acid. Compared to the bulk phase magnetization of 218 emu/g, the loss of magnetization, in our opinion, is not only due to the contribution from the surface oxide layer but also due to the existence of a nonmagnetic surface layer or spin cantings at the outer layer of the particles. However, the behavior of the 4.2 nm NPs is almost similar to the paramagnetic behavior at the applied field between 1 and 50 kOe, and the magnetization is not saturated even above 50 kOe. The magnetization at 50 kOe $M_{\text{at 50 kOe}}$, instead of saturation magnetization, is less than 32.0 emu/g. This may be due to a finite size effect or the formation of unknown Fe structures and needs to be further investigated in the future.

In summary, we have developed a facile large-scale synthesis method for monodisperse Fe nanoparticles by modest-temperature decomposition of iron carbonyl. The size can be well-controlled simply by varying the reaction parameters. For more than 8.0 nm Fe NPs, the saturation magnetization at 300 K was always above 150 emu/g, which proves that our method opens up a way to prepare gram quantities of monodisperse Fe NPs with high magnetization in a single reaction.

We thank Professor Shouheng Sun and Sara A. Majetich for helpful discussions and suggestions. This work was supported by NEDO program of Japan and the 21st Century COE Program of the MEXT project in Japan.

[1] S. Ohnuma, H. Fujimori, S. Mitani, and T. Masunoto, J. Appl. Phys. **79**, 5130 (1996).
[2] A. Inoue, T. Zhang, and H. Koshiba, J. Appl. Phys. **83**, 6326 (1998).
[3] T. W. Smith and D. Wychick, J. Phys. Chem. **84**, 1621 (1980).
[4] K. S. Suslick, M. Fang, and T. Hyeon, J. Am. Chem. Soc. **118**, 11960 (1996).
[5] D. Farrell, S. A. Majetich, and J. P. Wilcoxon, J. Phys. Chem. B **107**, 11022 (2003).
[6] C. H. Griffiths, M. P. O'Horo, and T. W. Smith, J. Appl. Phys. **50**, 7108 (1979).
[7] V. K. La Mer and R. H. Dinegar, J. Am. Chem. Soc. **72**, 4847 (1950).
[8] H. Reiss, J. Chem. Phys. **19**, 482 (1951).
[9] S. Sun and C. B. Murray, J. Appl. Phys. **85**, 4325 (1999).
[10] S. Sun, C. B. Murray, and H. Doyle, Mater. Res. Soc. Symp. Proc. **577**, 385 (1999).
[11] C. H. Griffiths, M. P. O'Horo, and T. W. Smith, J. Appl. Phys. **50**, 7108 (1979).
[12] M. W. Grinstaff, M. B. Salamon, and K. S. Suslick, Phys. Rev. B **48**, 269 (1993).